10. Lockwood, J. G., Is potential evapotranspiration and its relationship with actual evapotranspiration sensitive to elevated atmospheric CO_2 levels? *Climatic Change*, 1999, **41**, 193–212.
11. Yu, G. R., Wen, X. F., Sun, X. M., Tanner, B. D. and Lee, X. H., Overview of China flux and evaluation of its eddy covariance measurement. *Agric. For. Meteorol.*, 2006, **137**, 125–137.
12. Karimi, P. and Bastiaanssen, W. G. M., Spatial evapotranspiration, rainfall and land use data in water accounting – Part 1: Review of the accuracy of the remote sensing data. *Hydrol. Earth Syst. Sci. Discuss*., 2014, **11**, 1–51.
13. Tasumi, M., Trezza, R., Allen, R. G. and Wright, J. L., Operational aspects of satellite-based energy balance models for irrigated crops in the semi-arid US. *Irrig. Drain. Syst.*, 2005, **19**, 355–376.
14. Liou, Y. A. and Kar, S. K., Evapotranspiration estimation with remote sensing and various surface energy balance algorithms. a review. *Energies*, 2014, **7**, 2821–2849.
15. Saroj Sharma, M. P. and Prawasi, R., Geospatial approach cropping system analysis: a case study of Hisar district in Haryana. *Int. J. Comput. Technol. Appl.*, 2014, **5**, 457–461.
16. Bastiaanssen, W. G. M. and Roebeling, R. A., Analysis of land surface exchange processes in two agricultural regions in Spain using Thematic Mapper Simulator data. In Joint IAHS/IAMAP Symposium, Yokohama, Japan, IAHS, 11–23 July 1993, vol. 212, pp. 407–416.

ACKNOWLEDGEMENTS. We thank the Project Director, Water Technology Centre, Indian Agricultural Research Institute for providing the lysimeter data for validation of the SEBAL model.

Received 24 April 2016; revised accepted 6 February 2017

doi: 10.18520/cs/v113/i01/134-141

Numerical simulation of air-core vortex at intake

Behrouz Khadem Rabe[1,*], Seyyed Hossein Ghoreishi Najafabadi[1] and Hamed Sarkardeh[2]

[1]Department of Water and Environmental Engineering, Shahid Beheshti University, East Vafadar Blvd., Tehranpars, Tehran 167651719, Iran
[2]Department of Civil Engineering, Faculty of Engineering, Hakim Sabzevari University, Tohid Shahr, Sabzevar 9617976487, Iran

In order to study the features of vortex at horizontal intakes, numerical investigations have been performed. The tangential, radial, and axial distributions, and water surface profile were simulated to evaluate the flow behaviour and existence of an air-core vortex. The numerical results agree with existing experimental data. The correlation of vortex characteristics between numerical and experimental results was good. Regarding formed funnel profile of flow in the basin towards horizontal intake, its limits at the existence of an air-core vortex were analysed. The spiral flow pattern from surface towards intake was identified around the air-core vortex. This numerical simulation may help to get a deeper understanding in determining the submergence required to avoid air-entraining vortices in a reservoir.

Keywords: Air-core vortex, flow pattern, numerical simulation, velocity components, water surface profile.

FORMATION of free surface vortex at hydraulic intakes is an undesirable phenomenon. Engineers attempt to avoid formation of vortices in the vicinity of hydraulic facilities, because of severe technical difficulties that may arise. The features and strength of vortices are different and change with circumstances of flow and basin geometry[1]. In order to avoid problems arising from vortex formation at hydraulic intakes, better understanding of its mechanism will be helpful. One significant factor in vortex studies is the intake submergence, S which is defined as the distance between water surface and intake central axis[2]. Vortices are classified based on strength and shape into three different classes by Sarkardeh *et al.*[3].

Rankine[4] offered a mathematical model in which a rotating inner core of solid-body was bound by an outer zone of irrotational vortex motion. All vorticities were limited to the inner core zone and the outer zone was free of vorticity. During the last few decades, different studies experimentally modelled flow field in the presence of vortices to understand the behaviour of this phenomenon[3,5–18]. Besides experimental studies, researchers also tried to numerically simulate vortex formation in the reservoirs[19–27].

Despite such studies, there was no comprehensive numerical study on the characteristics of vortex flow with a strong air-core over a vertical intake. Indeed, in most of the earlier numerical studies, free surface vortex was simulated without air-core and little information was presented on the flow characteristics in a reservoir at the existence of an air-core vortex. This study aims to simulate spiral flow field towards a horizontal intake, analysing a 3D numerical model and verifying the results by experimental data.

Numerical simulation of vortex occurrence and surrounding flow shape in a tank was performed by solving three-dimensional Navier–Stokes equations of fluid motion based on finite volume method (FVM). Turbulence effects were modelled by large eddy simulation (LES) model. Cartesian grid also was used to mesh computational domain. By employing the fraction area/volume obstacle representation (FAVOR) method, walls, bed and vertical intake were defined as obstacles in the flow domain. The free surface was simulated by volume of fluid (VOF) method. Based on VOF method, cells

*For correspondence. (e-mail: b_khadem@sbu.ac.ir)

filled with water were indexed one, cells filled with air indexed zero, and cells having a proportion of water were assigned a value between zero and one based on the amount of water[28,29].

The general Navier–Stokes equations, governing continuity and kinematic of volume fraction, for incompressible fluid are

$$\partial(u_i A_i)/\partial x_i = 0, \quad (1)$$

$$\partial u_i/\partial t + (1/V_F)(u_j A_j \partial u_i/\partial x_j) = g_i - (1/\rho)(\partial P/\partial x_i) + [1/(\rho V_F)][\partial(A_j \tau_{ij})/\partial x_j], \quad (2)$$

$$\partial F/\partial t + (1/V_F)[\partial(F A_i u_i)/\partial x_i] = (1/V_F)[\partial(\upsilon_F A_i \partial F/\partial x_i)/\partial x_i], \quad (3)$$

where u_i (i = 1, 2, 3) represents the i-component of velocity; x_i is the i-coordinate in Cartesian coordinate system; V_F is volume fraction of fluid in each cell; A_i is fractional areas open to flow in the i-coordinate of Cartesian system; ρ is density; P is pressure; g_i is gravitational force in the subscript direction; ν_F is diffusion coefficient; F is the volume of fluid per unit volume and τ_{ij} characterizes the Reynolds stresses for which a turbulence model should be defined. LES turbulence model has been suggested[26,27], instead of other turbulence models as they do not represent the highly unstable and intermittent phenomenon such as a vortex, in a realistic way. For solving LES equations, Smagorinsky model is used and length scale is the local grid spacing.

Regarding free surface vortex formation, air entrainment should be simulated. In order to make air entrainment to occur, the turbulent kinetic energy per unit volume, P_t, must be larger than surface stabilizing forces of surface tension and gravity, P_d. The volume of air entrained per unit time, δV, is given below

$$\delta V = 0.5 A_s [2(P_t - P_d)/\rho]^{1/2} = 0.5 A_s [2(\rho k_T - \rho g_i L_t - \sigma/L_t)/\rho]^{1/2}, \quad (4)$$

where k_T is turbulent kinetic energy; A_s surface area; L_t characteristic size of turbulence eddies and σ is the coefficient of surface tension.

The geometry of flow field was defined based on the experimental model studies of Hite and Mih[10]. The cell size varied from 11 to 0.3 cm, corresponding to a non-uniform mesh size in x, y and z directions. Since the computing time is a limitation, it was necessary to find an adequate mesh size that can represent the expected phenomena to be analysed, in a reasonable processing time. Therefore, a sensitivity investigation was accomplished on mesh dimensions between 1, 0.5, 0.3 and 0.1 cm. Numerical results of tangential velocity for different mesh sizes were compared with theoretical formula which was presented by Rankine[4]. Mean deviation of results is presented in Table 1. Regarding approximations in obtaining theoretical formula, a 3 mm mesh size would appropriately simulate flow domain, while finer mesh size would significantly increase solution time.

In numerical simulations, it is important that the boundary conditions accurately represent physical processes. Based on FAVOR method, fluid flow domain was meshed along with obstacles. The tank body was simulated as a non-slip smooth surface. An upstream hydrostatic pressure was assigned and downstream of flow field was defined by volume flow rate. In order to consider the atmospheric pressure, a boundary condition at top with zero fluid fraction was implemented. The complete employed boundaries on the mesh block and their coordinate directions are shown in Table 2.

The incompressible fluid flow in this study is water with density of 1000 kg/m^3 and dynamic viscosity of 0.001 kg/m/s (at 20°C).

In order to validate the present numerical model, experimental model data of Hite and Mih[10] was used. The experiments were performed in a flume of 10.4 m length, 1.2 m width and 1.2 m depth (Figure 1). Water was pumped and the discharge was controlled with an inlet valve. The intake model was an opening on the flume side wall such that the approaching flow had to turn 90° to enter the intake.

Tangential, radial and axial velocities and water surface profile were presented and analysed in different parts to enable their comparison. Numerical simulation showed water surface depression above the intake as was detected in other experimental model studies (Figure 2)[30].

In the present numerical study, spiral motion at the vortex location (Figure 3) was simulated which was also

Table 1. Mean deviation of results

Mesh size (mm)	Mean deviation (%)
1	3.6
3	5.7
5	15.4
10	61.7

Table 2. Applied boundary conditions in model

Position	Type	Value
X-min	Wall	No slip
X-max	Pressure (fluid elevation)	0.82
Y-min	Volume flow rate	0.1512
Y-max	Wall	No slip
Z-min	Wall	No slip
Z-max	Pressure (fluid fraction)	0

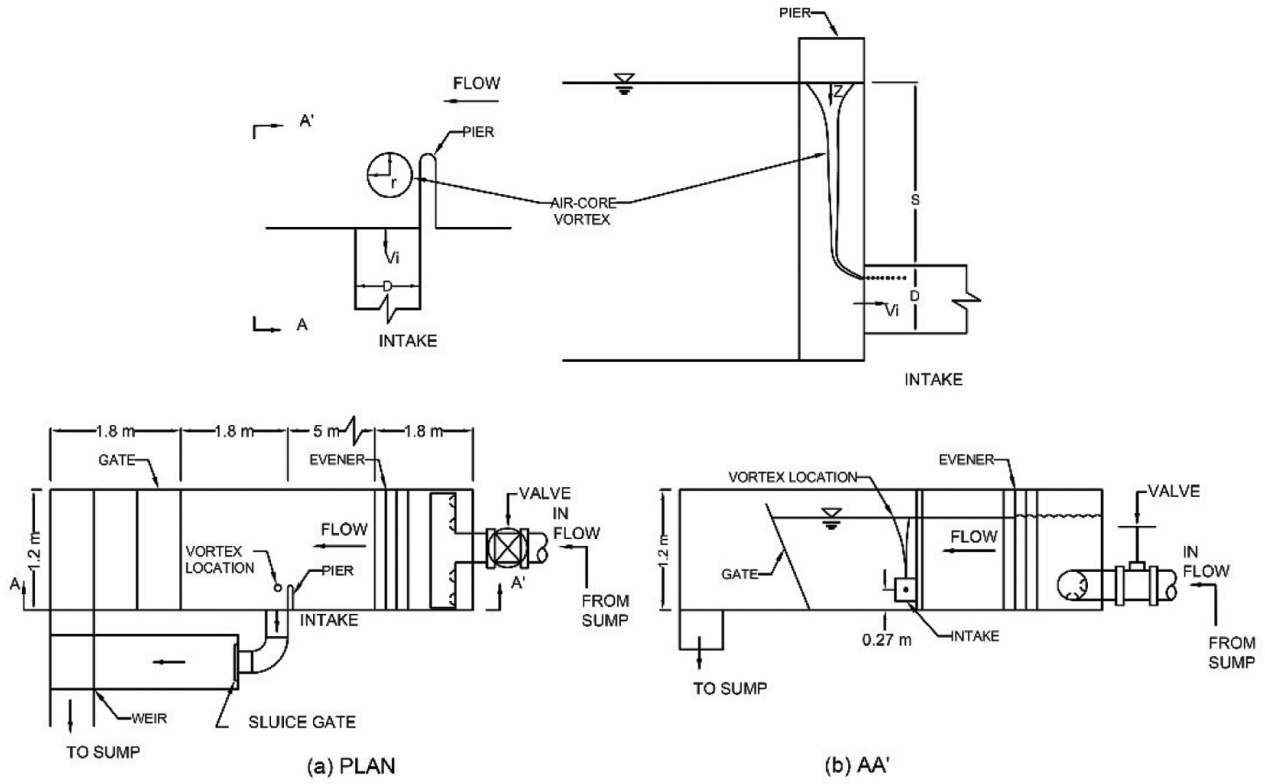

Figure 1. A schematic view of the model of Hite and Mih[10].

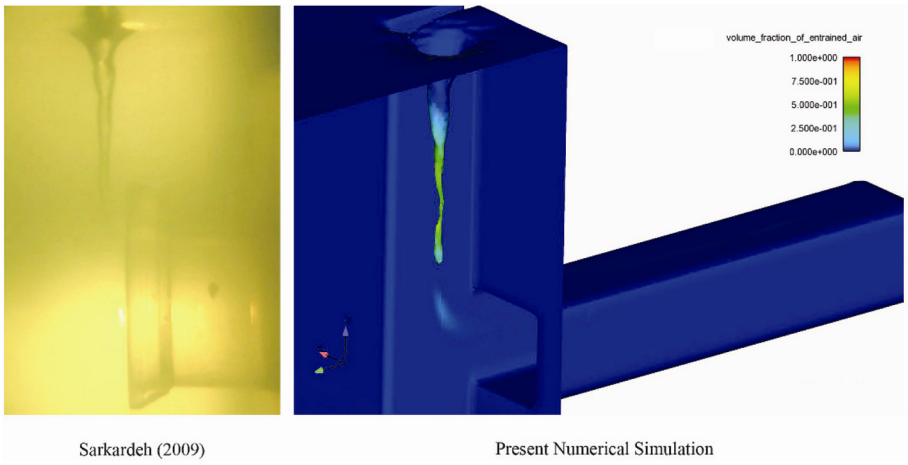

Figure 2. Water surface depression in numerical and experimental models.

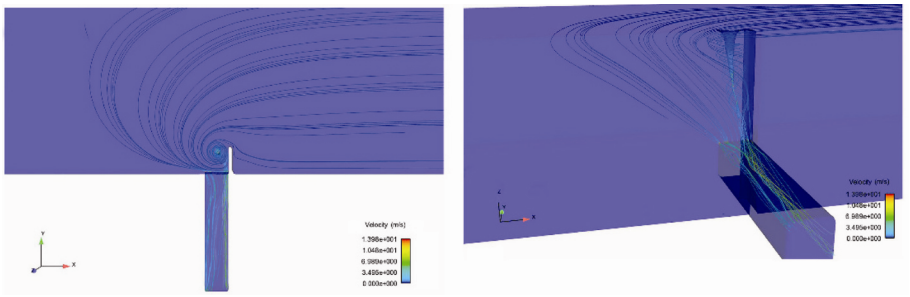

Figure 3. Spiral motion at the presence of simulated air-core vortex.

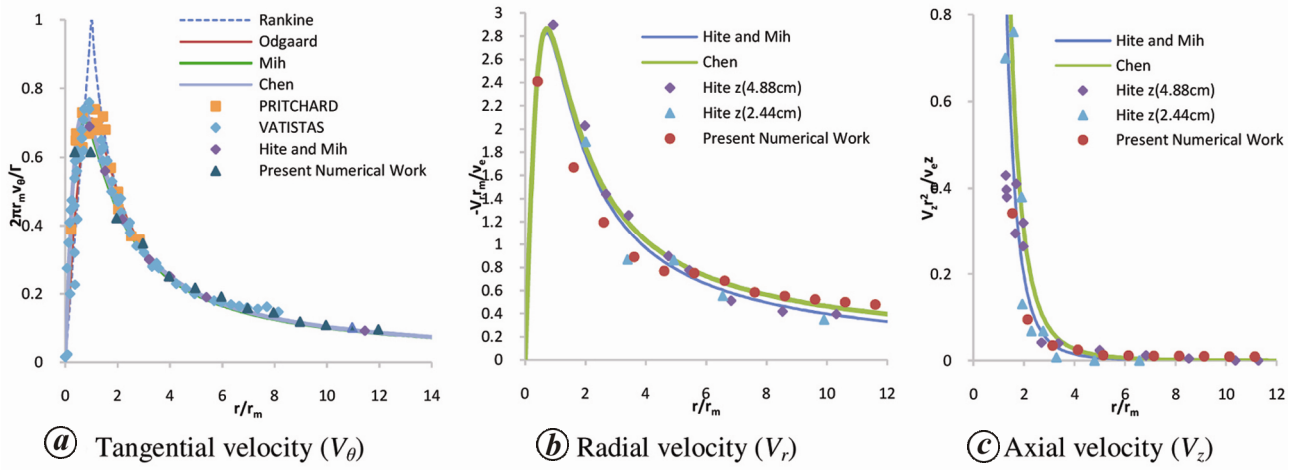

Figure 4. Velocity components.

Table 3. Previous studies on tangential velocity V_θ

Author	Year	Data	Approach
Rankine	1858	$r < r_m \quad v_\theta = \frac{\Gamma}{2\pi}\frac{r}{r_m^2}$	Analytical
		$r > r_m \quad v_\theta = \frac{\Gamma}{2\pi r}$	
Pritchard	1970	18 set tests	Experimental
Odgaard	1986	$v_\theta = \frac{\Gamma}{2\pi r}\left(1 - e^{-1.25\frac{r^2}{r_m^2}}\right)$	Analytical
Vatistas	1988	59 set tests	Experimental
Mih	1990	$v_\theta = \frac{\Gamma}{2\pi r_m}\frac{2(r/r_m)}{1+2(r/r_m)^2}$	Analytical
Hite and Mih	1994	41 set tests	Experimental
Chen *et al.*	2007	$V_\theta = \frac{\Gamma}{2\pi}\frac{2r}{r_m^2+2r^2}(1+az)$*	Analytical

*Γ = constant circulation of vortex outer zone, a = a coefficient independent of the variables r and z ($ah_1 = 2/e$).

Table 4. Previous studies on the radial velocity (V_r)

Author	Year	Data	Approach
Hite	1991	$V_r = -\frac{v_e}{r_m}\frac{8(r/r_m)}{1+2(r/r_m)^2}$	Analytical
Hite and Mih	1994	14 set tests	Experimental
Chen *et al.*	2007	$V_r = -v_e\frac{8r}{r_m^2+2r^2}[1+\ln(1+az)]$	Analytical

* v_e = eddy viscosity.

earlier proved theoretically, experimentally and numerically[27,31].

The experimental data indicated[10] that the velocity computed from Rankine's mathematical model was larger at r_m (radius at the maximum tangential velocity). Researchers proposed various models to estimate vortex behaviour. Some performed mathematical calculations with simplifying assumptions, while others performed experiments to understand vortex. Table 3 provides a summary of previous studies on tangential velocity. Results of previous studies are provided in Figure 4 *a* and compared with the present work.

Radial velocity causes fluid flow towards the centre of the vortex. To conserve angular momentum in the irrotational region, tangential velocity of the fluid must increase in consistent with the inverse function of the radius. To sustain motion of a steady vortex, it must have an inward radial velocity, otherwise, due to viscous action the tangential velocity will deteriorate[10]. Table 4 gives a brief summary of studies on radial velocity of vortices.

Figure 4 *b* compares the experimental and analytical data and provides numerical simulation. Hite experimental data agrees with the present numerical simulation.

The radial velocity changes to an axial velocity as it reaches the air–water boundary of the air-core. Hite and Mih[10] performed experiments on axial velocity. Hite and Mih[10] and Chen *et al.*[32] mathematically solved Navier–Stokes equations with simplified assumptions (Table 5). Figure 4 *c* shows that the present numerical simulation agreed with the measured experimental data. The maximum axial velocity will be equivalent to intake velocity. Therefore, v_z increases with depth Z up to intake velocity, and then it remains constant.

The water surface profile of a vortex drops hyperbolically from far field to half depth of water surface depression. It then decreases parabolically at the centre of the vortex[10]. Figure 5 shows that the present analytical results agree with experimental measurements of different researchers (Table 6).

To obtain accurate evaluation of the present numerical simulation, deviations of the results were compared with experimental and analytical data (Table 7). Results showed that in general, tangential velocity, radial velocity and water surface profile agreed with experimental and

Table 5. Previous studies on axial velocity (V_z)

Author	Year	Data	Approach
Hite	1991	$V_z = v_e \frac{z}{r_m^2} \frac{16}{[1+2(r/r_m)^2]^2}$	Analytical
Hite and Mih	1994	23 set tests	Experimental
Chen *et al.*	2007	$V_z = \frac{16 v_e r_m^2}{(r_m^2+2r^2)^2}\left[\frac{(1+az)}{a}\ln(1+az)\right]$	Analytical

Table 6. Previous studies on water surface profile

Author	Year	Data	Approach
Newman	1959	10 set tests	Experimental
Julien	1986	25 set tests	Experimental
Vatistas	1986	22 set tests	Experimental
Hite and Mih	1994	$\frac{H_r - H_0}{H} = \frac{2(r/r_m)^2}{1+2(r/r_m)^2}$	Analytical
Chen *et al.*	2007	$\frac{H_r - H_0}{h_1} = \frac{2r^2}{r_m^2+2r^2}(1+az)^2$ *	Analytical

*H_0 = water-surface elevation at the center, h_1 = total depth of air-core, H_r = water-surface elevation at r.

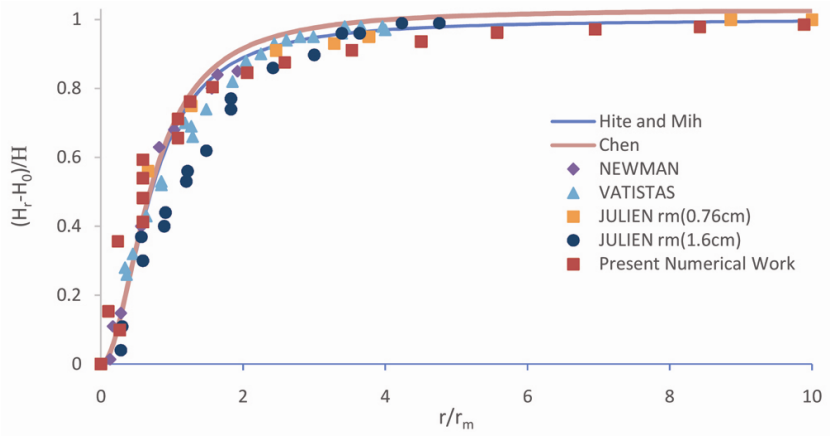

Figure 5. Water surface profile of vortex comparison.

analytical solutions, while axial velocity had more deviation. This was due to smaller axial velocity values. During numerical simulation, truncation of numbers is a common procedure to reduce the amount of data storage; hence, errors with small values of parameters arise. By refining mesh size this error may be decreased to some extent. Among velocity components, axial velocity has minimum influence on vortex behaviour, and usually ignored. In Table 7, we can clearly see that though axial velocity had more deviation from other studies, rest of the vortex parameters agreed with them. Results also showed that the numerical simulations fitted best with Chen *et al.*[32] analytical solution and Hite and Mih[10] experimental work.

Figure 6 shows a 3D view of the air-core vortex formed and stream lines in the reservoir. The numerical model demonstrates a conical air-core flow from water surface towards the intake. Spiral streamlines are seen over the intake in collaboration with air-core vortex. Results show a separate vertical flow to the intake in the form of a vertical cone. It can be concluded that the streamlines at the side boundary of this cone rotate spirally in friction with general horizontal funnel profile flow shape of basin towards the intake. It is because of the shear layer between the conical region at the top of the intake and horizontal funnel. Once the bulk of water in the dead region is low, it cannot resist the rotation of streamlines. Similar results were also presented by Sarkardeh *et al.*[27].

The vertical conical and horizontal funnel flow formed (Figure 7) shows that numerical results confirm this theory. According to this theory, reaching the upper stream lines

Table 7. Mean deviations between numerical simulation results and previous studies

Author	Year	Parameter	Approach	Mean deviation (%)
Rankine	1858	V_θ	Analytical	5.7
Newman	1959	H	Experimental	10.4
Pritchard	1970	V_θ	Experimental	2.4
Odgaard	1986	V_θ	Analytical	7.9
Julien	1986	H	Experimental	22.6
Vatistas	1986	H	Experimental	4.9
Vatistas	1988	V_θ	Experimental	3.1
Mih	1990	V_θ	Analytical	8.4
Hite	1991	V_r	Analytical	7.6
		V_z	Analytical	30.3
Hite and Mih	1994	V_θ	Experimental	6.4
		V_r	Experimental	1.7
		V_z	Experimental	28.5
		H	Analytical	10.1
Chen *et al.*	2007	V_θ	Analytical	5.2
		V_r	Analytical	2.2
		V_z	Analytical	9.6
		H	Analytical	7.6

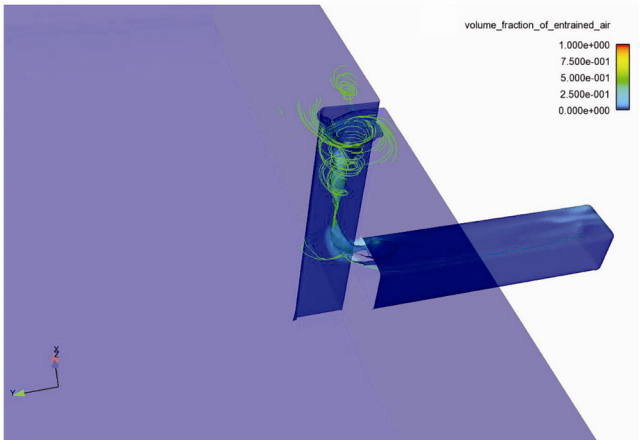

Figure 6. Streamlines around an air-core vortex.

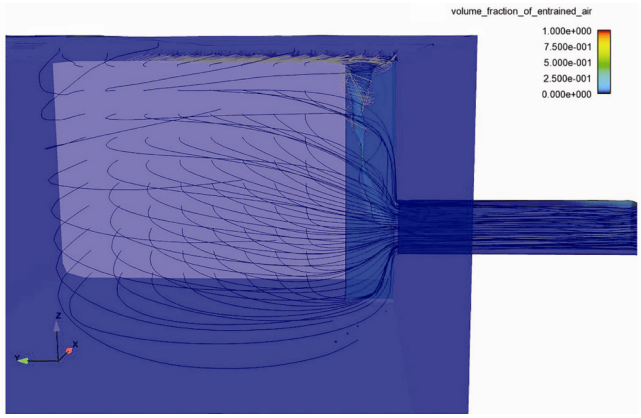

Figure 7. 3D streamlines in the reservoir at the presence of an air-core vortex.

of a high velocity zone (horizontal funnel flow) in the reservoir to the water surface, is the beginning of the vertical conical flow from surface to the intake. It can be noted that decreasing S/D (relative submergence) or increasing intake Fr (Froude number) accelerate reaching of upper stream lines of the horizontal funnel flow to the water surface and initiate rotation of the weaker zone (water surface). Vorticities and rotations form along the interaction boundary between the horizontal funnel and vertical conical zones. A surface vortex with an air-core will form due to contraction of vorticities at the intake entrance.

In the present numerical simulation, free surface vortex with air-core and flow characteristics along the spiral motion in the reservoir was analysed. The experimental data were also used to verify the numerical results. Numerical results for tangential, radial, axial velocities and water surface profile were validated using experimental and mathematical data of the reservoir. Results showed that in general, tangential and radial velocities, and water surface profile correlated well with experimental data and analytical solutions, while axial velocity had more deviation. Numerical simulation results of tangential velocity of air-core free surface vortex, deviated about 5% and 6% from analytical solutions by Chen *et al.*[32] and experimental tests by Hite and Mih[10] respectively. Radial velocity results deviated about 2% and 1.5% from analytical solutions by Chen *et al.*[32] and experimental tests by Hite and Mih[10] respectively. Numerical simulation exposed a horizontal funnel shape and a vertical conical flow towards the intake. Furthermore, spiral streamlines perceived over the intake followed up to the location of the vortex in the model. It was determined that reaching of upper stream lines of the horizontal funnel flow to the water surface, will cause a rotation at the water surface. Some parameters accelerate this condition such as decreasing intake submerged depth or increasing intake Froude number. Thus the results of the

present numerical research give an appropriate vision towards air-core free surface vortices and flow pattern surrounding it.

1. Sarkardeh, H., Zarrati, A. R., Jabbari, E. and Roshan, R., Discussion of prediction of intake vortex risk by nearest neighbors modeling. *ASCE J. Hydraul. Eng.*, 2012, **137**(6), 701–705; doi: 10.1061/(ASCE)HY.1943-7900.0000344.
2. Knauss, J., *Swirling Flow Problems at Intakes*, A. A. Balkema, Rotterdam, Netherlands, 1987.
3. Sarkardeh, H., Zarrati, A. R. and Roshan, R., Effect of intake head wall and trash rack on vortices. *J. Hydraul. Res.*, 2010, **48**(1), 108–112; doi:10.1080/00221680903565952.
4. Rankine, W. J. M., *A Manual of Applied Mechanics*, Richard Griffin and Co., London, England, 1858.
5. Amiri, S. M., Zarrati, A. R., Roshan, R. and Sarkardeh, H., Surface vortex prevention at power intakes by horizontal plates. *J. Water Manage. (ICE)*, 2011, **164**(4), 193–200; doi:10.1680/wama.1000009.
6. Ansar, M. and Nakato, T., Experimental study of 3D pump-intake flows with and without cross flow. *ASCE J. Hydraul. Eng.*, 2001, **127**(10), 825–834; doi:10.1061/(ASCE)0733-9429(2001)127:10(825).
7. Camnasio, E., Orsi, E. and Schleiss, A. J., Experimental study of velocity fields in rectangular shallow reservoirs. *J. Hydraul. Res.*, 2011, **49**(3), 352–358; doi:10.1080/00221686.2011.574387.
8. Carriveau, R., Kopp, G. and Baddour, R., Stretching-sustained intake vortices. *J. Hydraul. Res.*, 2009, **47**(4), 486–491; doi:10.1080/00221686.2009.9522024.
9. Chen, Z., Ettema, R. and Lai, Y., Ice-tank and numerical study of frazil ingestion by submerged intakes. *ASCE J. Hydraul. Eng.*, 2004, **130**(2), 101–111; doi:10.1061/(ASCE)0733-9429(2004)130:2(101).
10. Hite, J. E. and Mih, W., Velocity of air-core vortices at hydraulic intakes. *ASCE J. Hydraul. Eng.*, 1994, **120**(3), 284–297; doi: 10.1061/(ASCE)0733-9429(1994)120:3(284).
11. Khanarmuei, M. R., Rahimzadeh, H. and Sarkardeh, H., Investigating the effect of intake withdrawal direction on critical submergence and strength of vortices. *Modares Mech. Eng.*, 2014, **14**(10), 35–42 (in Persian).
12. Odgaard, J. A., Free-surface air core vortex. *ASCE J. Hydraul. Eng.*, 1986, **112**(7), 610–620; doi:10.1061/(ASCE)0733-9429(1986)112:7(610).
13. Roshan, R., Sarkardeh, H. and Zarrati, A. R., Vortex study on hydraulic model of Godar-e-Landar Dam and hydropower plant. In Fifth International Conference on Computational and Experimental Methods in Multiphase and Complex Flow, UK, 2009, vol. 63, pp. 217–225; doi:10.2495/MPF090191.
14. Sarkardeh, H., Jabbari, E., Zarrati, A. R. and Tavakkol, S., Velocity field in a reservoir in the presence of an air-core vortex. *J. Water Manage. (ICE)*, 2013, **164**(4), 193–200, doi:10.1680/wama.13.00046.
15. Taghvaei, S. M., Roshan, R., Safavi, K. H. and Sarkardeh, H., Anti-vortex structures at hydropower dams. *Int. J. Phys. Sci.*, 2012, **7**(28), 5069–5077; doi: 10.5897/IJPS12.387.
16. Yildirim, N., Eyüpoğlu, A. and Taştan, K., Critical submergence for dual rectangular intakes. *ASCE J. Energy Eng.*, 2012, **138**(4), 237–245; doi:10.1061/(ASCE)EY.1943-7897.0000073.
17. Azarpira, M., Sarkardeh, H., Tavakkol, S., Roshan, R. and Bakhshi, H., Vortices in dam reservoir: a case study of Karun III dam. *Sadhana*, 2014, **39**(5), 1201–1209; doi:10.1007/s12046-014-0252-7.
18. Khanarmuei, M. R., Rahimzadeh, H., Kakuei, A. R. and Sarkardeh, H., Effect of vortex formation on sediment transport at dual pipe intakes. *Sadhana*, 2016, **41**(9), 1055–1061; doi:10.1007/s12046-016-0531-6.
19. Constantinescu, G. S. and Patel, V. C., Numerical model for simulation of pump-intake flow and vortices. *ASCE J. Hydraul. Eng.*, 1998, **124**(2), 123–134; doi:10.1061/(ASCE)0733-9429(1998)124:2(123).
20. Constantinescu, G. S. and Patel, V. C., Role of turbulence model in prediction of pump-bay vortices. *ASCE J. Hydraul. Eng.*, 2000, **126**(5), 387–391; doi: 10.1061/(ASCE)0733-9429(2000)126:5(387).
21. Teklemariam, E., Korbaylo, B. W., Groeneveld, J. L. and Fuchs, D. M., Computational fluid dynamics: diverse applications in hydropower project's design and analysis. In CWRA 55th Annual Conference, Winnipeg, Canada, 2002, pp. 1–20.
22. Marghzar, S. H., Montazerin, N. and Rahimzadeh, H., Flow field, turbulence and critical condition at a horizontal water intake. *Proc. Inst. Mech. Eng. A: Power Energy*, 2003, **217**(1), 53–62; doi:10.1243/095765003321148691.
23. Suerich-Gulick, F., Gaskin, S., Villeneuve, M., Holder, G. and Parkinson, E., Experimental and numerical analysis of free surface vortices at a hydropower intake. In Seventh International Conference Hydroscience and Engineering (ICHE), USA, 2006, pp. 1–11.
24. Okamura, T., Kyoji, K. and Matsui, J., CFD prediction and model experiment on suction vortices in pump sump. In Proceedings of the 9th Asian International Conference Fluid Machinery, Korea, 2007, pp. 1–10.
25. Abir, I., Annie-Claude, B. and Gerard, B., Numerical simulation of flow field formed in water pump sump. In 24th Symposium Hydraulic Machinery and Systems, Argentina, 2008, pp. 1–11.
26. Lucino, C., Liscia, S. and Duró, G., Vortex detection in pump sumps by means of CFD. XXIV Latin American Congress on Hydraulics, Punta Del Este, Uruguay, 2010, pp. 1–12.
27. Sarkardeh, H., Zarrati, A. R., Jabbari, E. and Marosi, M., Numerical simulation and analysis of flow in a reservoir in the presence of vortex. *J. Eng. Appl. Comput. Fluid Mech.*, 2014, **8**(4), 598–608; doi:10.1080/19942060.2014.11083310.
28. Hirt, C. W. and Nicholes, B. D., Volume of fluid (VOF) method for the dynamics of free boundaries. *J. Comput. Phys.*, 1981, **39**, 201–225; doi:10.1016/0021-9991(81)90145-5.
29. Hirt, C. W. and Sicilian, J. M., A porosity technique for the definition of obstacles in rectangular cell meshes. Proceedings of the 4th International Conference on Ship Hydrodynamics, National Academy of Science, Washington, DC, 1985, pp. 1–19.
30. Sarkardeh, H., Effect of Reservoir Vortex on Flow Condition in Power Tunnels. M Sc thesis. Amirkabir University of Technology (Tehran Polytechnic), Tehran, Iran (in Persian), 2009.
31. Lugt, H. J., *Vortex Flow in Nature and Technology*, John Wiley & Sons, New York, USA, 1983.
32. Chen, Y. L., Wu, C., Ye, M. and Ju, X., Hydraulic characteristics of vertical vortex at hydraulic intakes. *J. Hydrodyn.*, 2007, **19**(2), 143–149; doi:10.1016/S1001-6058(07)60040-7.

Received 16 August 2016; revised accepted 19 January 2017

doi: 10.18520/cs/v113/i01/141-147